

Coulomb localization and exchange modulation in two-electron coupled quantum dots

Dmitriy V. Melnikov, Ahmed Taha[†], Nahil Sobh[†], and Jean-Pierre Leburton

Beckman Institute for Advanced Science and Technology,

University of Illinois at Urbana-Champaign, 401 North Mathews Avenue, Urbana, IL 61801

[†]*National Center for Supercomputing Applications,*

University of Illinois at Urbana-Champaign, 1205 West Clark Street, Urbana, IL 61801

(Dated: April 18, 2006)

A general study of the singlet-triplet energy separation (exchange energy) in the two-electron system confined in a realistic double quantum dot system is performed using a hybrid multiscale approach where the many-body Schrödinger equation is solved exactly within the full quantum dot device environment. The exchange energy is computed as a function of the gate confinement and magnetic field. It is found, in particular, that at zero magnetic field the exchange energy varies from meV to sub- μeV value as the confinement gate biases (tunneling barrier) are changed and the system is driven from a single quantum dot to two coupled quantum dots. The small values of the exchange coupling in this structure are attributed to the large inter-electron separation arising when the Coulomb repulsion dominates tunneling.

PACS numbers: 73.21.La, 73.21.-b

Recently, solid state systems based on coupled quantum dots [1] have attracted considerable attention as promising candidates for the practical realization of spin-based quantum computation [2]. In these structures fundamental quantum logic gates (such as C-NOT gate) can be realized by manipulating the entanglement of a two-electron pair. The interaction between the two electron spins (or qubits) can be quantified by computing the exchange energy J , *i.e.*, the difference between the lowest singlet and triplet states [3].

Two laterally coupled quantum dots (QD), where the confinement of individual electrons can be achieved electrostatically by changing the voltages applied to gate electrodes, offer sufficiently large degree of tuning to perform the basic quantum logic operations. Among possible experimental systems, two vertical mesa-structures, each containing one QD, coupled in a lateral direction have recently been investigated [4]. In another one [5–7], a two-dimensional (2D) electron gas formed at about 100 nm below the surface can be effectively depleted by the gates on top of the structure, so that electrons can be added to the QD system one by one by regulating the applied gate biases. In particular, for this type of double QD structure, values of the tunnel coupling ranging from $\sim 10 \mu\text{eV}$ to $\sim 250 \mu\text{eV}$ have been measured [6, 7].

In this work we concentrate on the study of the electron coupling in the symmetric configuration of the double QD system, *i.e.*, identical voltages are applied to the left and right QDs. This symmetric structure is well suited for qubits manipulation in a stable way at low magnetic fields. Previous works published on this subject almost always resorted to model potentials to describe the QD confinement and evaluate the exchange coupling using either analytical approaches valid in the limits of weak [8, 9] and strong [10] coupling between the QDs or perform fully numerical calculations using the density-functional theory [11] or the exact diagonalization technique [12, 13]. While model potentials are useful

in establishing general trends in the behavior of the inter-electron coupling, they usually fall short in reproducing quantitatively the properties of real systems without *a priori* knowledge of the QD device structure [14].

In order to accurately evaluate the exchange energy in realistic double QD systems by taking into account full quantum device environment (gates geometry, varying doping, different layer materials, etc.), in the present work we employ a hybrid multiscale method in which the single-electron confinement potential is obtained from the self-consistent solution of the 3D Poisson equation with device boundary conditions [15]:

$$\nabla [\epsilon(\mathbf{r})\nabla\phi(\mathbf{r})] = 4\pi\rho(\mathbf{r}), \quad (1)$$

where $\epsilon(\mathbf{r})$ is the dielectric constant of the media and $\rho(\mathbf{r})$ is the charge density in the regions outside the QD system (the QDs are unpopulated at this stage)

$$\rho(\mathbf{r}) = e [N_D^+(\mathbf{r}) - N_A^-(\mathbf{r}) + p(\mathbf{r}) - n(\mathbf{r})] \quad (2)$$

obtained from the semi-classical Thomas-Fermi electron $n(\mathbf{r})$ and hole $p(\mathbf{r})$ densities screened by the ionized donors and acceptors with concentrations $N_D^+(\mathbf{r})$ and $N_A^-(\mathbf{r})$. In this work we simulated the experimental structure of Ref. [5, 16] (which appears to have a similar top gate layout to other systems [7]), though we expect that our general conclusions should remain applicable to other structures as well.

The electrostatic potential $\phi(\mathbf{r})$ obtained in this way is responsible for electrons confinement in the QD region, and as such, is used in the direct numerical diagonalization of the two-particle Hamiltonian \hat{H} [17]:

$$\hat{H} = \sum_{i=1}^2 \hat{h}_i + \frac{e^2}{\epsilon|\mathbf{r}_1 - \mathbf{r}_2|}, \quad (3)$$

where the single-particle Hamiltonians $\hat{h}(\mathbf{r}_i)$ are

$$\hat{h}_i = -\frac{\hbar^2}{2m^*} \left(\nabla_i - \frac{ie}{\hbar c} \mathbf{A}_i \right)^2 + \phi(\mathbf{r}_i), \quad (4)$$

and the last term represents the Coulomb interaction between electrons. Here m^* and ε are the electron effective mass and dielectric constant of GaAs, while $\mathbf{A} = (1/2)(Bx, -By, 0)$ is the vector potential in the symmetric gauge for the magnetic field \mathbf{B} oriented perpendicular to the lateral xy plane in which QDs are coupled.

In order to diagonalize Eqs. (3,4), the corresponding wave functions are expanded in the basis set of the anisotropic harmonic oscillator states which lead to the dense matrices (the filling factor is $\sim 30\%$). Throughout the work, the basis set size required to accurately evaluate the exchange energy is varied from the lowest 8×8 states in the single QD regime to 13×13 in the case of two virtually decoupled QDs. To handle such large expansions, the parallel processing is used to solve generalized Hermitian eigenvalue problems.

As the electron density is strongly localized in the direction perpendicular to the xy plane with extension of about 20 nm [16], we make an additional simplification by considering a 2D cut of the full 3D potential $\phi(\mathbf{r})$ through the maximum of the wave function in the vertical direction, thus making the Hamiltonian \hat{H} effectively two-dimensional. Nevertheless, as this 2D potential is obtained from the full 3D calculations, it already incorporated image charge effects from the gates. On the other hand, polarization of the environment outside the QD region caused by the electrons inside is neglected as this contribution is expected to be very small because of (1) the electrons in QDs are well separated from the outside charges by the electrostatic barriers created by the gates, which also effectively deplete the QD region from the mobile charges, and (2) we are primarily interested in the energy differences between the two spin states so that constant background effects cancel out [18].

By varying the left and right gate voltages $V_L = V_R$ while keeping the rest of the gates at fixed voltages (top and middle gates are at -0.6 V while both plungers are set to zero [16]), the system is changed from a "large" single QD formed in the center of the structure at $V_L = V_R = -2.0$ V to two coupled smaller QDs with an interdot separation of about 150 nm and a tunnel barrier of about 1.5 meV at $V_L = V_R = -0.5$ V (Fig. 1). At -2.0 V [Fig. 1(a)], the potential has an approximately elliptic shape with confinement strengths $\hbar\omega_x \approx 2.1$ meV and $\hbar\omega_y \approx 2.8$ meV and the minimum (dark blue region) located in the center of the structure around $x \sim 0$ and $y \sim 0$. The electrons are prevented from leaking in the outside regions by the left/right gates (red regions) and by constrictions between the left/right and top gates (light blue region). When the left/right gate voltages are made more positive, the tunnel barrier between the two QDs finally emerges at about $V_L = V_R \approx -0.8$ V, and the overall confinement potential profile in the QD region achieves a "bow tie" (or butterfly) shape with the inversion symmetry in the x direction only [Fig. 1(b)].

Such significant changes in the confinement potential geometry exert a large effect on the exchange energy as

well as other quantities of interest as can be evidenced from the data obtained at zero magnetic field and shown in Fig. 2. In Fig. 2(a) as $V_L = V_R$ is swept from -2.0 to -0.55 V, the exchange energy J (red curve) changes dramatically, by more than three orders of magnitude, from ~ 0.5 meV to about $0.12 \mu\text{eV}$. At the same time, the difference between the two lowest single-particle states, $2t$, which would give the exchange energy in the non-interacting system of two electrons, exhibits a much slower decrease from ≈ 2 meV to $\approx 69 \mu\text{eV}$ (blue curve [19]). This interval of $2t$ values overlaps with energy range found experimentally for the inter-dot coupling strengths [6, 7]. The large disparity between the values of $2t$ and J demonstrates the rising importance of the Coulomb repulsion in the system when the inter-dot distance is increased and electrons in both singlet and triplet states become localized in the individual QDs. This is also confirmed by the inspection of the electron density plots [Fig. 2(b)], where one notices that the distance between the two density maxima is significantly smaller (or the overlap is larger) in the case of two non-interacting electrons. It is also clearly seen in these plots that electrons in the triplet state are farther from each other which is physically due to the Pauli principle that tends to pull same spin particles apart.

The exchange energy in magnetic fields is plotted in Fig. 3 for different voltages. It is seen that with increasing voltage (decreasing inter-dot coupling), the values of the exchange energy decrease as expected, and J becomes negative at about 1.5 T in the single dot regime. This transition point (the so-called singlet-triplet transition, STT) gradually shifts to ~ 1 T when the voltage becomes more positive and the QDs decouple. The decrease can be explained by the rising influence of the Coulomb interaction compared to the single-particle effects [13]. From the results displayed in Fig. 3(b), one also deduces that the ratio of $J(B = 0)$ to the exchange energy (magnitude) at its minimum (negative) value is much larger in the double-dot regime (~ 8 at $V_L = V_R = -0.7$ V vs. ~ 3 at $V_L = V_R = -2.0$ V), *i.e.*, the negative J region become suppressed, similarly to the situation in single elliptic QDs [17] and model double dot systems [13].

The decrease in the exchange coupling is accompanied by smaller values of the double occupancy probability P_{DO} or the probability of finding two singlet electrons at the same side of the structure (or in one QD in the double-dot range of voltages). For the purposes of quantum computation, the exchange energy should be as large as possible while the P_{DO} should be kept small. One can see from Fig. 4 that in this structure, this quantity decreases progressively from $\sim 50\%$ in the single dot case to $\sim 0.8\%$ for the double QD configuration. In magnetic fields, it also exhibits a fairly sharp drop at about 2 T to 20% in the former case, while the latter case is characterized by a more gradual decay due to the increasing electron localization in separate QDs. The sharp drop at $V_L = V_R \approx -2.0$ V is due to the transition between s -like and p -like single-particle states analogous to tran-

sitions between states with different angular momenta in the circular QD geometry [13, 21].

Including Zeeman interaction in the Hamiltonian (3) leads to a lowering of the triplet energy by about 25 $\mu\text{eV}/\text{T}$, thereby strongly affecting our results only in the limit of the weak inter-dot coupling where the STT shifts from 1 T to about 20 mT. Despite its small value, this field is still higher than the local magnetic fields arising from the GaAs nuclear spins $B_{nuc} \sim 3$ mT [22], thus making the experimental observation of this transition feasible. However, the exchange energy obtained for $V_L = V_R = -0.55$ V is comparable to the Zeeman splitting induced by B_{nuc} which effectively mixes singlet and triplet states, and as such, direct measurement of this energy in this voltage interval can be difficult, if ever possible. In this regard, one should also mention that the results presented in this work are to some extent the "best case" scenario. We have also performed simulations using different top and middle gate biases ($V_T < V_M$) and obtained exchange energy values which are much smaller than the data reported here (primarily because different biases applied to top and middle gates

lower the overall symmetry of the confinement potential in the y -direction and lead to the smaller constriction between the constituent QDs).

To conclude, we have calculated the exchange energy of the two-electron system confined in a realistic double QD structure by the numerically exact diagonalization of the corresponding Schrödinger equation within the full quantum device environment. We found that owing to the large interdot separation, the exchange energy achieves *vanishingly* small values even in the absence of an appreciable tunneling barrier between the two QDs, *i.e.*, it is the Coulomb repulsion rather than the weak tunneling through the barrier that localizes electrons in individual dots.

This work was supported by DARPA QuIST program DAAD19-01-1-0659, Strategic Applications Program at NCSA, and the Material Computational Center (MCC). The work performed at the MCC was supported by the NSF grant DMR-03 25939 ITR, with additional support through the Frederick Seitz Materials Research Laboratory (USDE grant DEFG02-91ER45439) at the University of Illinois at Urbana-Champaign.

-
- [1] L. P. Kouwenhoven, D. G. Austing, and S. Tarucha, Rep. Progr. Phys. **64**, 701 (2001); S. M. Reimann and M. Manninen, Rev. Mod. Phys. **74**, 1283 (2002).
- [2] A. Galindo and M. A. Martín-Delgado, Rev. Mod. Phys. **74**, 347 (2002).
- [3] D. Loss and D. P. DiVincenzo, Phys. Rev. A **57**, 120 (1998).
- [4] T. Hatano, M. Stopa, and S. Tarucha, Science **309**, 268 (2005).
- [5] J. M. Elzerman, R. Hanson, J. S. Greidanus, L. H. Willems van Beveren, S. De Franceschi, L. M. K. Vanderstypen, S. Tarucha, and L. P. Kouwenhoven, Phys. Rev. B **67** 161308(R) (2003).
- [6] W. G. van der Wiel, S. De Franceschi, J. M. Elzerman, T. Fujisawa, S. Tarucha, and L. P. Kouwenhoven, Rev. Mod. Phys. **75**, 1 (2003); T. Hayashi, T. Fujisawa, H. D. Cheong, Y. H. Jeong, and Y. Hirayama, Phys. Rev. Lett. **91**, 226804 (2003); A. K. Hüttel, S. Ludwig, H. Lorenz, K. Eberl, and J. P. Kotthaus, Phys. Rev. B **72**, 081310(R) (2005).
- [7] J. R. Petta, A.C. Johnson, C. M. Marcus, M. P. Hanson, and A. C. Gossard, Phys. Rev. Lett. **93**, 186802 (2004); M. Pioro-Ladrière, R. Abolfath, P. Zawadzki, J. Lapointe, S. A. Studenikin, A. S. Sachrajda, and P. Hawrylak, Phys. Rev. B **72**, 125307 (2005).
- [8] G. Burkard, D. Loss, and D. P. DiVincenzo, Phys. Rev. B **59**, 2070 (1999).
- [9] X. Hu and S. Das Sarma, Phys. Rev. A **61**, 062301 (2000).
- [10] W. Dybalski and P. Hawrylak, Phys. Rev. B **72**, 205432 (2005).
- [11] A. Wensauer, O. Steffens, M. Suhrke, and U. Rössler, Phys. Rev. B **62**, 2605 (2001); H. Saarikoski, E. Räsänen, S. Siljamäki, A. Harju, M. J. Puska, and R. M. Nieminen, Eur. Phys. J. B **26**, 241 (2002).
- [12] A. Harju, S. Siljamäki, and R. M. Nieminen, Phys. Rev. Lett. **88**, 226804 (2002); B. Szafran, F. M. Peeters, and S. Bednarek, Phys. Rev. B **70**, 205318 (2004).
- [13] D. V. Melnikov and J.-P. Leburton, Phys. Rev. B **73**, 155301 (2006).
- [14] S. Nagaraja, J.-P. Leburton, and R. M. Martin, Phys. Rev. B **60**, 8759 (1999).
- [15] D. V. Melnikov, Ph. Matagne, J.-P. Leburton, D.G. Austing, G. Yu, S. Tarucha, J. Fettig, and N. Sobh, Phys. Rev. B **72**, 085331 (2005).
- [16] L.-X. Zhang, P. Matagne, J.-P. Leburton, R. Hanson, and L. P. Kouwenhoven, Phys. Rev. B **69**, 245301 (2004).
- [17] D. V. Melnikov and J.-P. Leburton, Phys. Rev. B **73**, 085320 (2006).
- [18] Because of the 2D approximation, and in order to obtain general results, calculations here were conducted without utilizing the common Fermi level of the QD system.
- [19] Note that the two curves for the single-particle energy separation are very close to one another, thus validating our assumption about the use of a 2D potential (3D calculations give rise to an increase in the exchange energy values that do not exceed 15 %, consistent with our earlier results for single QDs [17]).
- [20] Our calculations characterizing the individual QDs in the structure give the following results: the electron addition energy to the individual QD is 4.2 meV, single particle excitation energy is 1.7 meV, the exchange energy is 0.5 meV at zero magnetic field and the STT is at about 1 T, all of which are in a reasonable agreement with available experimental measurements [5].
- [21] M. Wagner, U. Merkt, and A. V. Chaplik, Phys. Rev. B **45**, R1951 (1992).
- [22] J. R. Petta, A.C. Johnson, J. M. Taylor, E. A. Laird, A. Yacoby, M. D. Lukin, C. M. Marcus, M. P. Hanson, and A. C. Gossard, Science **309**, 2180 (2005).

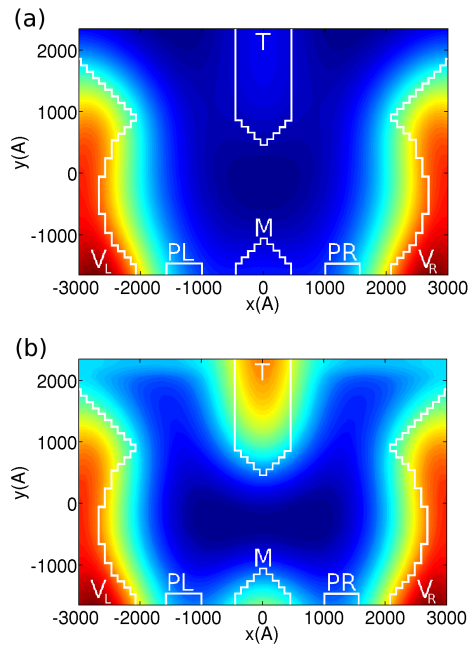


FIG. 1: (Color online) Confinement potential in the QD region at $V_L = V_R = -2.0$ V (a) and at $V_L = V_R = -0.5$ V (b). The white contours show the discretized top gate layout. Symbols T, M, PL and PR stand for top, middle, left and right plunger gates, respectively.

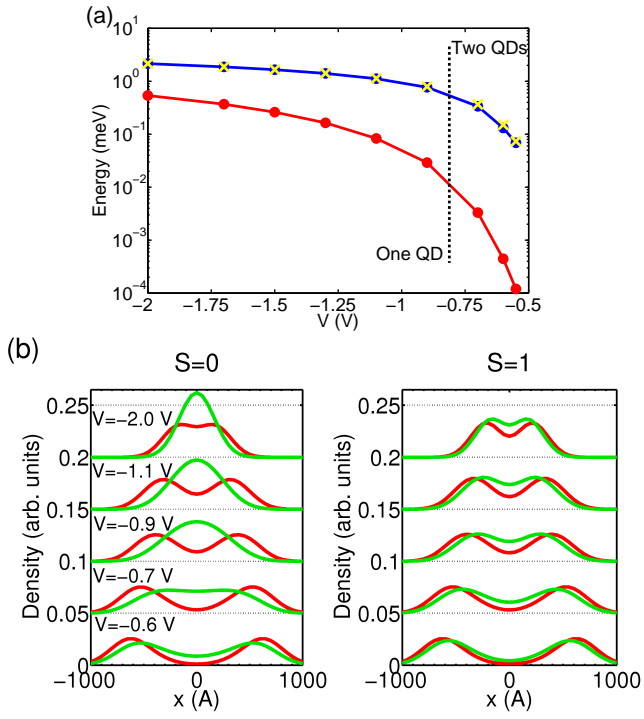


FIG. 2: (Color online) (a) Exchange energy J (red) and the tunnel coupling $2t$ (blue) as functions of the left/right gate bias $V = (V_L = V_R)$ at zero magnetic field. Blue curve is the result of the present hybrid approach while the yellow symbols (\times) give the values of $2t$ obtained from the 3D calculations [15, 19]. (b) Electron density for the interacting (red) and non-interacting (green) electrons in the singlet ($S = 0$) and triplet ($S = 1$) states for $V = V_L = V_R = -2.0$ V, -1.1 V, -0.9 V, -0.7 V, -0.6 V.

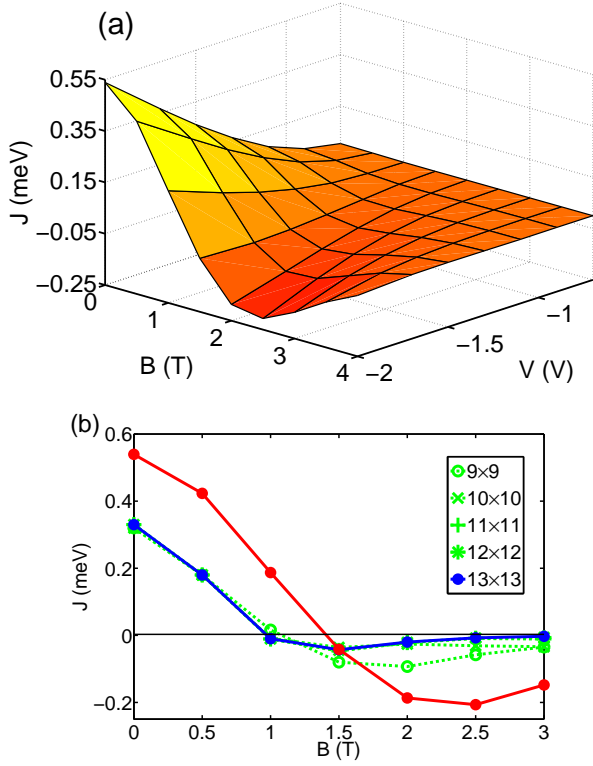


FIG. 3: (Color online) (a) Exchange energy J as a function of the left/right gate bias $V = (V_L = V_R)$ in the magnetic field B ; (b) J vs. B at $V_L = V_R = -2.0$ V (red) and $V_L = V_R = -0.7$ V (blue). For the latter case, the values of J are multiplied by 10^2 to bring them to scale. Also, for this case several curves computed with different number of basis states (dashed green curves) are also shown to demonstrate the convergence in the exchange energy values.

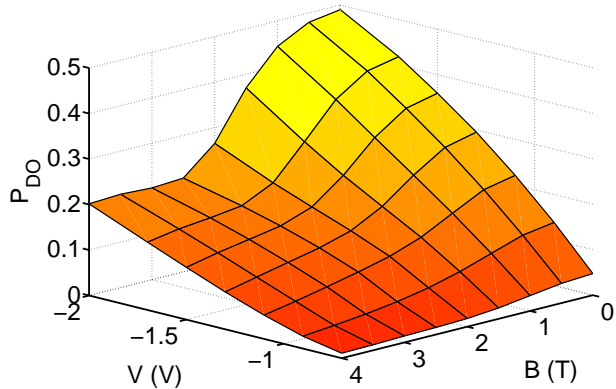


FIG. 4: (Color online) Double occupancy probability P_{DO} vs. the left/right gate voltage $V = (V_L = V_R)$ and the magnetic field B .